RSC Advances

RSC Publishing

PAPER

View Article Online
View Journal | View Issue

Cite this: *RSC Adv.*, 2013, **3**, 26382

Recognition between V- and dumbbell-shaped molecules†

Wing-Yan Wong,[a] Siu-Fung Lee,[a] Hoi-Shan Chan,[a] Thomas C. W. Mak,[a] Chi-Hin Wong,[b] Lau-Shan Huang,[b] J. Fraser Stoddart*[c] and Ken Cham-Fai Leung*[bd]

A series of 2,6-bis(imino)pyridyl-based V-shaped compounds bearing various *para*-substituents on the terminal aromatic rings [$C_5H_3N(CH{=}N{-}C_6H_4R)_2$; R = OMe, ^{i}Pr, Me, H, Cl, F, and CF_3] have been prepared and investigated for their reversible binding with the dumbbell-shaped cations NH_2^+–{CH_2–C_6H_3(OMe-3,5)$_2$}$_2$ and 9-anthryl–CH_2–NH_2^+–CH_2–C_6H_3(OMe-3,5)$_2$. Three crystalline V-shaped compounds and a dumbbell hexafluorophosphate were characterised in the solid state by X-ray structural analysis. The binding mode of the 1 : 1 V-shaped molecule·dumbbell complexes was evaluated by ^{1}H NMR spectroscopy. The binding constants (90–400 M^{-1} in dichloromethane) and stoichiometries of the complexes were determined using the Method of Continuous Variations and the Rose-Drago Method based on ^{1}H NMR spectroscopic data. In a series of V-shaped compounds, the binding strength with both dumbbell cations diminishes with the decreasing electron-donating ability of the R substituents. Specifically, one of the diimine V-shaped compounds shows a stronger binding with the symmetrical dumbbell than with the unsymmetrical anthracene-containing dumbbell. Fluorescence measurements of equimolar mixtures of the V-shaped compounds and the unsymmetrical dumbbell have revealed a reduced anthracene emission which is approximately 50% that of the original intensity. Rapid and complete dissociation (<5 min) of the V-shaped compounds from the dumbbells was realised using an excess of acid or base, whereas only partial dissociation of the complexes was achieved with a large excess of water (<1 h).

Received 9th July 2013
Accepted 18th October 2013

DOI: 10.1039/c3ra43470b

www.rsc.org/advances

1. Introduction

The term molecular clip or tweezer was coined by Whitlock[1] to describe a class of synthetic receptors which contain two pre-organised aromatic chromophores covalently linked by a single spacer. Apropriate spacers allow molecular clips to form sandwich complexes with aromatic substrates employing π–π stacking interactions. More sophisticated molecular clips carry additional functional groups oriented towards their clefts, so that hydrogen bonding and electrostatic interactions can provide some synergy when binding appropriate substrates. These acyclic receptors possess distinct advantages over their cyclic relatives—*e.g.*, cyclophanes—owing to their pre-organised cavities and topologies which account for their wide application for binding neutral and cationic aromatic substrates.[2–4]

About a decade ago, Park *et al.*[5] reported a Schiff-base molecular clip which forms a 1 : 1 complex with salicylaldehyde with an association constant (log K_a) of 1.10 in acetonitrile. The complex formation was monitored by ^{1}H NMR titration of the Schiff-base clip with salicylaldehyde. The driving forces for complex formation are hydrogen bonding and π–π stacking interactions between the aromatic faces. Other types of clips, which display pH-dependent reversible binding of complexes,[6] exhibit guest-exchange behaviour,[7] enable recognition of macro-molecular sequences,[8] and serve as drug carriers,[9] have appeared in the recent literature.

In general, conformationally induced self-assembly[10] between a structurally post-organised compound and a substrate will render a rapid change of physical properties (solubility, organic functionality, *etc.*) of the substrate, and the association process can, in principle, be reversible. There exist only a few reports, however, on the dissociation of self-assembled complexes induced by various stimuli. A recent dissociation study of a dynamic [2]rotaxane showed that an acyclic diimine exhibits relative stability in the presence of an ammonium dumbbell in a competitive mixture.[11] This phenomenon has prompted us to find out how substituents on relatively rigid

[a]*Department of Chemistry, The Chinese University of Hong Kong, Shatin, NT, Hong Kong SAR, P.R. China*

[b]*Department of Chemistry and Institute of Creativity, The Hong Kong Baptist University, Kowloon Tong, Kowloon, Hong Kong SAR, P.R. China*

[c]*Department of Chemistry, Northwestern University, 2145 Sheridan Road, Evanston, Illinois 60208, USA*

[d]*Institute of Molecular Functional Materials, University Grants Committee, Hong Kong SAR, P.R. China. E-mail: stoddart@northwestern.edu; cfleung@hkbu.edu.hk*

† Electronic supplementary information (ESI) available. CCDC 798464, 784761–784763. For ESI and crystallographic data in CIF or other electronic format see DOI: 10.1039/c3ra43470b

diimine V-shaped compounds affect their binding affinities and photophysical properties.[11] In the present investigation, self-assembly[10,12] and effective dissociation[13] between selected 2,6-bis(imino)pyridyl (diimine) V-shaped compounds and dumbbell substrates have been demonstrated. Systematic exploration of these readily cleavable molecular recognition processes may point the way to rapid functionalisation and disfunctionalisation of polyelectrolyte materials, such as polycationic polymers and nanoparticles. V-shaped compounds may be useful for designing 2,6-bis(imino)pyridyl transition metal-based polymerization catalysts.[14] Furthermore, they have been designed and engineered to form Borromean rings[15] and metal–organic frameworks (MOFs).[16]

2. Results and discussion

2.1. Design and synthesis

Two dumbbell-like diimine salts,[11,13b] **1**-H·PF_6 and **2**-H·PF_6 (Fig. 1), were selected for investigation. The use of **1**-H·PF_6 allows the formation of V·dumbbell complexes for convenient characterisation and comparison of the stereoelectronic effects of dumbbell upon the binding event. On the other hand, the anthracene-containing dumbbell **2**-H·PF_6 permits the formation of complexes with various V-shaped compounds with enhanced aromatic interactions that can be characterised conveniently by fluorescence spectroscopy. A series (Fig. 1) of 2,6-bis(imino)pyridyl diimine V-shaped compounds **3–9** with various *para*-substituents on the terminal aromatic rings were synthesised. The stoichiometries and binding constants of the V-shaped compounds with two dumbbells were determined by monitoring the chemical shift changes in their ^{1}H NMR spectra. The fluorescence properties of the complexes formed between the V-shaped compounds and the dumbbell **2**-H·PF_6 were also monitored. It is reasonable to expect that the self-assembly between V-shaped compounds and the dumbbells is facilitated by (i) significant electrostatic interactions between the dumbbell's secondary dialkylammonium centre (–$^+NH_2$–) and the V-shaped molecules' N atoms, (ii) hydrogen bonding between the –CH_2–NH_2^+–CH_2– segment of the dumbbells and the V-shaped molecules' N atoms, and (iii) any π–π interactions involving the aromatic rings.[17]

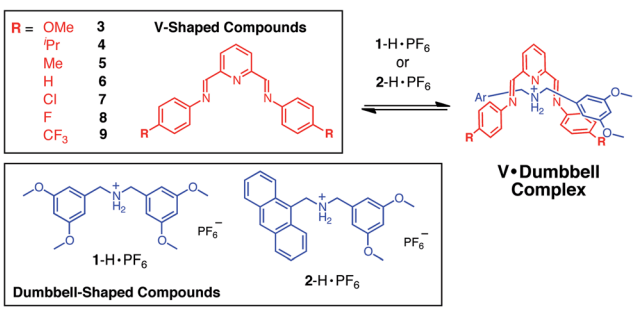

Fig. 1 Structural formulae of the 2,6-bis(imino)pyridyl (diimine) V-shaped compounds **3–9**, the symmetrical dumbbell **1**-H·PF_6, the unsymmetrical dumbbell **2**-H·PF_6, and the self-assembly of V·Dumbbell complex.

Dumbbell compounds **1**-H·PF_6 and **2**-H·PF_6 were prepared according to literature procedures.[11,13b] The V-shaped compounds **3–9** were synthesised in high yields by condensation of 2,6-diformylpyridine with the corresponding R-substituted aniline (1 : 2 molar ratio) in the presence of molecular sieves (4 Å). Diimine V-shaped compounds **4**, **7**, **8**, and **9** are all new compounds. The V·dumbbell complexes were formed by mixing stochiometric amounts of the V-shaped compound and the dumbbell in a solvent mixture containing CH_2Cl_2 and MeCN at concentrations of approximately 20–120 mM. It was confirmed by ^{1}H NMR spectroscopy that equilibration to form complexes is complete within 10 minutes.

2.2 Characterisation of components

2.2.1 ^{1}H NMR spectroscopy. All the diimine V-shaped compounds were characterised by ^{1}H NMR spectroscopy in CD_2Cl_2. The V-shaped compounds, dumbbells, and their complexes are well solvated in CH_2Cl_2, which is neither sufficiently acidic to catalyse the hydrolysis of the imino groups, nor influential enough to affect electron donor–acceptor interactions. Even although a very small amount of water is inevitably present in the ^{1}H NMR samples, all the diimine V-shaped compounds showed no residual aldehyde signal at δ = 10.15 ppm in their NMR spectra, indicating that they are thermodynamically stable. The imine proton resonances of the V-shaped compounds show gradual changes in the chemical shifts according to the nature of electron-withdrawing and electron-donating substituents. Compared to the reference compound **6** (R = H), the imine protons of the more electron-withdrawing group-substituted V-shaped compounds **7–9** (R = Cl, F, CF_3) reveal upfield shifts, while the more electron-donating substituted V-shaped compounds **3–5** (R = OMe, ^{i}Pr, Me) show downfield shifts (Table 1).

2.2.2 Mass spectrometry. The new V-shaped compounds **4**, **7**, **8**, and **9** were analysed by high-resolution matrix-assisted laser desorption ionization-time-of-flight-mass spectrometry (MALDI-TOF-MS). All mass spectra show the presence of the expected molecular plus sodium ion peaks without any fragmentation of the hydrolysed imine V-shaped compounds or 2,6-diformylpyridine. It follows that these compounds possess remarkable stabilities in the gas phase.

2.2.3 X-Ray crystallography. The crystal structures of the dumbbell **2**-H·PF_6, and the V-shaped compounds **3**, **5** and **8**

Table 1 Comparison of chemical shift of imine signal in the ^{1}H NMR spectra of V-shaped compounds **3–9** at 296 K in CD_2Cl_2

V-shaped compound	R group substitution	Chemical shift of imine proton δ (ppm)
3	OMe	8.68
4	^{i}Pr	8.68
5	Me	8.66
6	H	8.66
7	Cl	8.63
8	F	8.64
9	CF_3	8.64

were obtained following X-ray diffraction analysis (Fig. 2 and 3). Single crystals of **2**-H·PF_6 were obtained by slow vapour diffusion of ^{t}BuOMe into a solution of **2**-H·PF_6 in $ClCH_2CH_2Cl$. In the solid state structure (Fig. 2) of **2**-H·PF_6, two adjacent dumbbell molecules are in contact with each other with their anthracene planes lying nearly perpendicular to one another. The shortest distance between a hydrogen atom of one anthracene moiety and the plane of the other anthracene moiety is 2.99 Å, providing evidence for a moderate C–H···π interaction.[18] Single-crystal X-ray analyses (Fig. 3) of the free V-shaped molecules reveal that they have relaxed linear shapes, with the pyridyl and imine nitrogen atoms orientated on opposite sides of the molecules.

2.3 Characterisation of V·Dumbbell complexes

All attempts to grow single crystals of V·dumbbell complexes by slow vapour diffusion of an equimolar mixture of the components in CH_2Cl_2 or MeCN or $ClCH_2CH_2Cl$ with ^{t}BuOMe were unsuccessful. Consequently, the V·dumbbell complexes were characterised by ^{1}H NMR spectroscopy, mass spectrometry, and UV/visible absorption and fluorescence spectroscopies.

2.3.1 ^{1}H NMR spectroscopy. The V-shaped compounds **3–9** and the two dumbbells **1**-H·PF_6 and **2**-H·PF_6 were mixed and matched (1 : 1 ratio, 20 mM), and left for 6 h to reach equilibrium before recording their ^{1}H NMR spectra. From all the ^{1}H NMR spectra of the V·dumbbell complexes, proton signals of free and complexed V-shaped molecules appeared as weighted-averages, suggesting that all complexation/decomplexation is fast on the ^{1}HNMR timescale. Complex formation can be detected by the pronounced shifts of signals in the ^{1}H NMR spectra of dumbbells after addition of the V-shaped compounds. By way of an example, for an equimolar mixture of the V-shaped compound **3** and the dumbbell **2**-H·PF_6 (Fig. 4), significant shifts in the resonances for protons (H_d, H_e, H_i, H_l, H_m, and H_n) signify the emergence of intermolecular N^+–H···N and N^+C–H···N hydrogen bonding, π–π stacking, and electrostatic interactions on complexation.[19] Noticeably, an aldehyde proton signal at $\delta = 10.09$ ppm is present since a small amount of **3** inevitably underwent hydrolysis in the presence of the acidic dumbbell **2**-H·PF_6.

Upon complexation, the imine nitrogen atoms and pyridine unit on the V-shaped compound donate electrons to the ammonium centre of the dumbbells and, in return, disperse the electron density around the imine. Therefore, by monitoring the extent of upfield shift of the resonance for the imine proton, the binding strength between the V-shaped compound and the dumbbell can be estimated. From Table 2, the imine proton upfield shifts decrease down the series of complexes, suggesting a gradual decline in the binding strength. Furthermore,

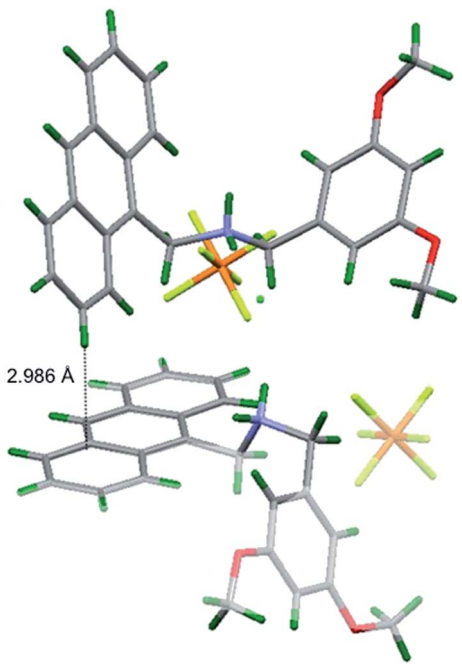

Fig. 2 Molecular packing in the crystal structure of the dumbbell **2**-H·PF_6. Atom colour key—red: oxygen; violet; nitrogen; yellow: fluorine; orange: phosphorus; grey: carbon; and green: hydrogen.

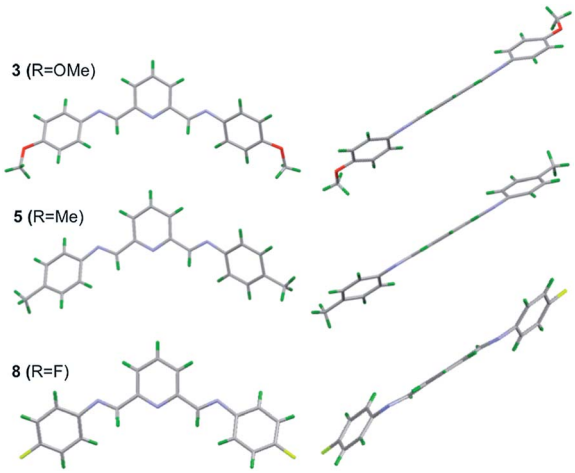

Fig. 3 Different views of the conformations of the V-shaped compounds **3** (R = OMe), **5** (R = Me), and **8** (R = F) from their respective crystal structures. Atom colour key—red: oxygen; violet: nitrogen; yellow: fluorine; grey: carbon; and green: hydrogen.

Table 2 Comparison of upfield shift of the imine ^{1}H NMR signal in the V-shaped compounds after complexation with equimolar quantities of the dumbbells **1**-H·PF_6 and **2**-H·PF_6

		Upfield shift of imine proton $\Delta\delta$ (ppm)[a]	
V-shaped compound	R	Dumbbell **1**-H·PF_6	Dumbbell **2**-H·PF_6
3	OMe	0.06	0.13
4	^{i}Pr	0.06	0.13
5	Me	0.05	0.09
6	H	0.03	0.10
7	Cl	0.01	0.06
8	F	0.01	0.06
9	CF_3	0.01	0.03

[a] $\Delta\delta = \delta_{obs} - \delta$; where δ_{obs} is the observed imine proton signal in the fast equilibrating mixture and δ is the imine proton signal of the free V-shaped compounds.

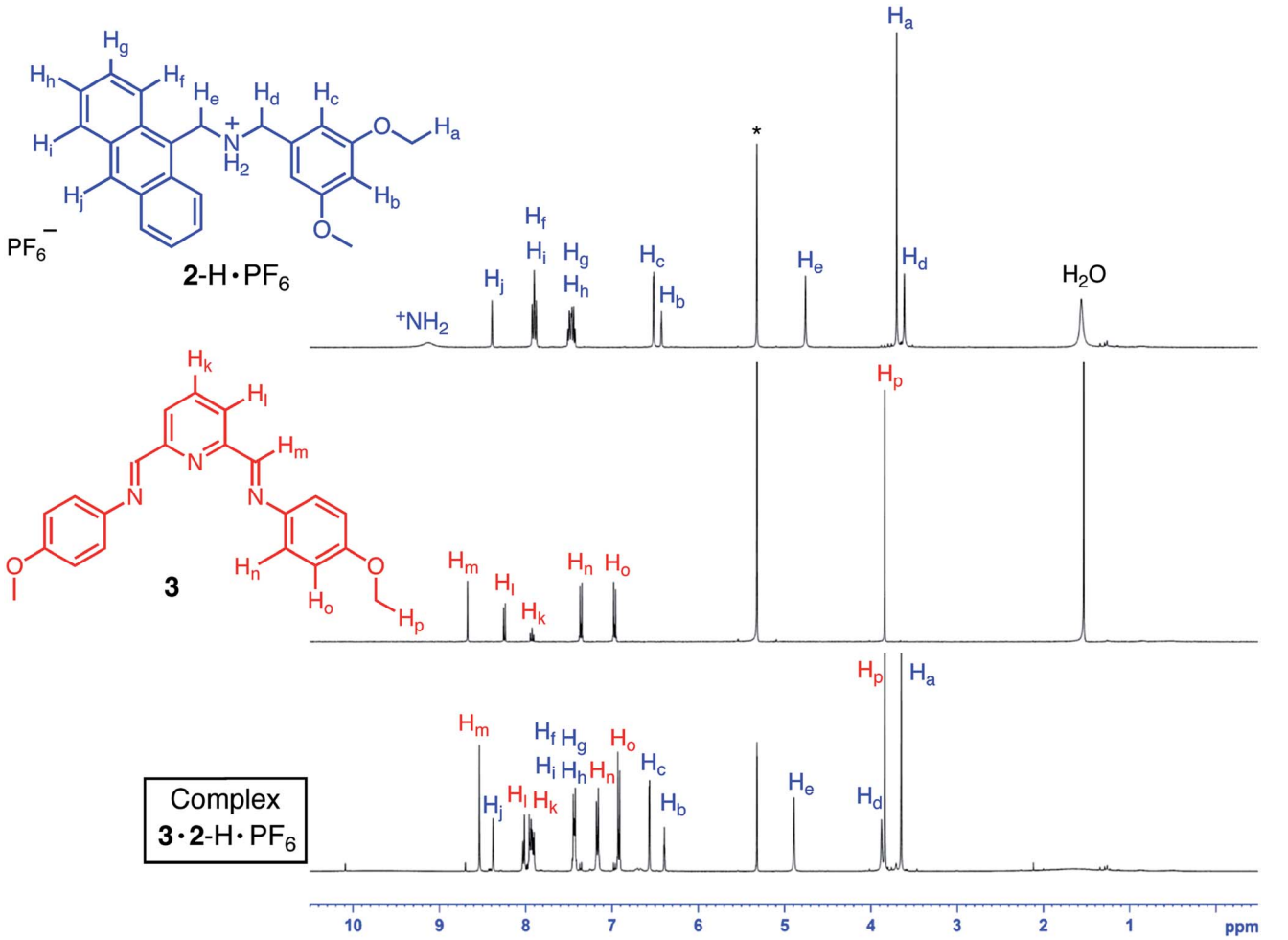

Fig. 4 Stacked partial ^{1}H NMR spectra of the dumbbell **2**-H·PF_6, the V-shaped compound **3** and the equimolar mixture of **2**-H·PF_6 and **3** in CD_2Cl_2. Asterisk denotes the solvent residual signal.

complexes formed with the dumbbell **2**-H·PF_6 show (Fig. S3†) greater shifts than the corresponding complexes with **1**-H·PF_6. The greater binding strength may be attributed to additional π–π stacking interactions provided by the anthracene moiety of **2** H·PF_6.

In order to investigate the geometry of the V·dumbbell complexes, two-dimensional NOESY ^{1}H NMR spectroscopy was employed. From an equimolar mixture of the V-shaped compound **3** and the dumbbell **2**-H·PF_6 in dry CD_2Cl_2, the resonances for protons H_d and H_e, which are located next to the ammonium centre of the dumbbell, shift significantly (Fig. S1† and Table 3). Moreover, the resonances for the protons H_l, H_n, and H_m, which constitute the aryl protons and the imine proton of the V-shaped compound, shift significantly as well. Hence, the electronic environments of these moieties are drastically altered upon complexation.

Furthermore, strong nuclear Overhauser effect (NOE) signals appear (Fig. S1† and Table 3) among the dumbbell protons H_c (with H_p and H_n), H_d (with H_o), and H_j (with H_k and H_l). Protons on the dumbbell H_a, H_b, and H_{e-i} do not show any correlations with the protons of the V-shaped compound, while the imine proton H_m also shows no correlation with any dumbbell

Table 3 Comparison of the ^{1}H NMR signal shift of the V·dumbbell complex **3**·**2**-H·PF_6. Significant signal shifts were observed for protons H_d, H_e, H_l, H_m, and H_n (Italic). D denotes the dumbbell **2**-H·PF_6 while V denotes the V-shaped compound **3**

Proton	Uncomplex δ (ppm)	Complexed δ (ppm)	Δδ (ppm)	Correlation
H_a (D)	3.70	3.64	0.06	—
H_b (D)	6.42	6.38	0.04	—
H_c (D)	6.51	6.56	0.05	H_p (V), H_n (V)
H_d (D)	3.61	3.87	*0.26*	H_o (V)
H_e (D)	4.76	4.89	*0.13*	—
H_f (D)	7.91	7.95	0.04	—
H_g (D)	7.49	7.44	0.05	—
H_h (D)	7.44	7.42	0.02	—
H_i (D)	7.89	7.91	0.02	—
H_j (D)	8.39	8.37	0.02	H_k (V), H_l (V)
H_k (V)	7.93	7.98	0.05	H_j (D)
H_l (V)	8.25	8.02	*0.23*	H_j (D)
H_m (V)	8.68	8.53	*0.15*	—
H_n (V)	7.36	7.16	*0.20*	H_c (D)
H_o (V)	6.97	6.92	0.05	H_d (D)
H_p (V)	3.84	3.84	0.00	H_c (D)

Table 4 Comparison of the ^{1}H NMR signal shift of the V·dumbbell complex **3**·**1**-H·PF_6. Significant signal shifts were observed for protons H_c', H_d', H_l, and H_n (Italic). D denotes the dumbbell **1**-H·PF_6 while V denotes the V-shaped compound **3**

Proton	Uncomplex δ (ppm)	Complexed δ (ppm)	$\Delta\delta$ (ppm)	Correlation
H_a' (D)	3.74	3.65	0.09	—
H_b' (D)	6.40	6.35	0.05	—
H_c' (D)	6.66	6.54	*0.12*	H_n (V)
H_d' (D)	3.88	4.06	*0.18*	—
H_k (V)	7.93	8.02	0.09	—
H_l (V)	8.25	8.02	*0.23*	—
H_m (V)	8.68	8.62	0.06	—
H_n (V)	7.36	7.22	*0.14*	H_c' (D)
H_o (V)	6.97	6.97	0.00	—
H_p (V)	3.84	3.85	0.01	—

protons. Therefore, it is reasonable to conclude that the V-shaped compound's three N atoms are in close proximity to the dumbbell's ammonium centre, thereby forming the V-shaped dumbbell complexes, stabilised by electrostatic interactions and hydrogen bonding.

Two-dimensional NOESY ^{1}H NMR spectroscopy was employed to investigate an equimolar mixture of V-shaped compound **3** and the dumbbell **1**-H·PF_6 in dry CD_2Cl_2. The aryl protons H_c' and methylene protons H_d' of the dumbbell, as well as the aryl protons H_l and H_n of the V-shaped compound, shift significantly (Fig. S2,† Table 4). Again, the electronic environments of these moieties are altered considerably upon complexation. Strong NOE signals appear only for H_c' on the dumbbell and H_n of the V-shaped compound. Other protons show no correlation. This observation provides further evidence that the V-shaped compound's three N atoms are in close proximity to the dumbbell's ammonium centre. Based on the $\Delta\delta$ values, the V·dumbbell complex **3**·**2**-H·PF_6 possesses enhanced binding interactions compared with that of the V·dumbbell complex **3**·**1**-H·PF_6.

Attempts to determine binding constants (K_a), as well as stoichiometries of the complexes formed between the V-shaped compounds **3–9** and the dumbbells **1**-H·PF_6 and **2**-H·PF_6, have been made by ^{1}H NMR titration experiments. The total concentration of the solution was kept constant while the ratio between the V-shaped compound and the dumbbell was varied. The dependence of complexation-induced ^{1}H NMR shifts of methylene protons adjacent to the ammonium centres on the dumbbells was monitored as the mole fraction of dumbbell was varied. The stoichiometries were determined from the *x*-coordinate at the maximum in a Job plot.[20] Complexation between V-shaped compound **5** and the dumbbell **1**-H·PF_6 is taken as an example (Fig. S8†). Extrapolation of data points near the mole fractions of 0 and 1 gave an interception point at a mole fraction of 0.51. Therefore, V-shaped compound **5** and the dumbbell **1**-H·PF_6 form a 1 : 1 complex. Since the chemical shift of the methylene protons adjacent to the ammonium centre of the complexed dumbbell δ_c cannot be obtained directly, the Rose-Drago method[21] was applied to evaluate the complex concentration and hence the binding constant (K_a). By fitting the data to a 1 : 1 complexation model, δ_c and K_a were determined (Table S1†) to be 4.10 ppm and 360 M^{-1}, respectively. For instance, the complexation between **4** and **1**-H·PF_6 revealed a binding constant of 400 M^{-1}, a value that is comparable with that of a pre-organised crown ether-based complexation.[17b] Some of the complexes, however, especially those with the dumbbell **2**-H·PF_6, are unstable and can exist in several co-conformations as a result of varying the mole fractions of the complexes. Thus, large errors arose during the calculation and their Job plots could not be obtained.

2.3.2 Mass spectrometry. Mixtures of V-shaped compounds **3–9** with the dumbbells **1**-H·PF_6 and **2**-H·PF_6 in dry CH_2Cl_2 (total conc. = 0.02 mM) were prepared according to the stoichiometries obtained from the Job plots and analysed (Table S2†) with high resolution ESI-MS. It transpires that the

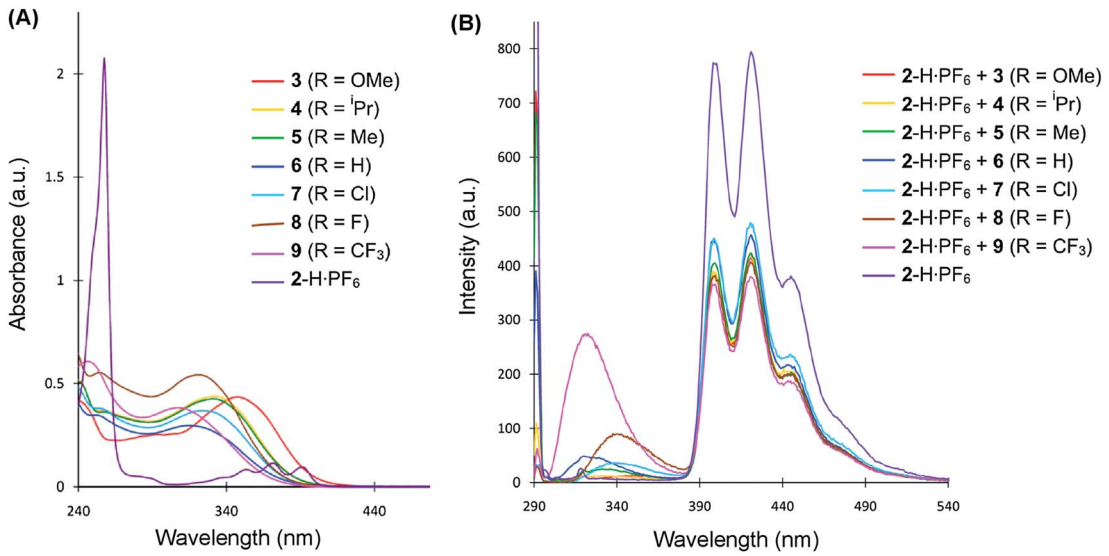

Fig. 5 (A): UV/visible absorption spectra of the V-shaped compounds **3–9** and the dumbbell **2**-H·PF_6 (0.02 mM in CH_2Cl_2). (B): Fluorescence emission spectra (excitation wavelength = 290 nm) of the dumbbell **2**-H·PF_6 and its equimolar mixture with the V-shaped compounds **3–9** (0.02 mM in CH_2Cl_2).

1 : 1 molecular V-shaped compound/dumbbell ratio is the most stable co-conformation in the gas phase. All the detected 1 : 1 V-shaped molecule/dumbbell molecular ions agree well with their calculated values.

2.3.3 Absorption and fluorescence spectroscopies. The UV/visible absorption spectra (Fig. 5A) of all the V-shaped compounds show a broad imino residual band, while the spectrum of the dumbbell 2-H·PF_6 shows the characteristic anthracene absorption band at 300–400 nm. Since the dumbbell 1-H·PF_6 does not have significant fluorescent properties, attention has been focused on the anthracene-containing dumbbell 2-H·PF_6. The fluorescence spectra (excitation at 290 nm, fixed dumbbell concentration to 0.02 mM) of equimolar mixtures of the V-shaped compounds 3–9 and the dumbbell 2-H·PF_6 show (Fig. 5B) the characteristic anthracene emission (λ_{max} = 418 nm), yet with lower intensities than that of the free 2-H·PF_6. This result suggests that, although the binding strengths of V-shaped compounds are not strong enough to quench 2-H·PF_6 completely, they are able to lower the original intensity of the anthracene emission by approximately 50%. This result agrees well with the previous NMR spectroscopic investigation wherein it was shown that the binding strength decreases down the series.

2.4 Dissociation of V·Dumbbell complexes

In a further set of experiments, complexes **4·1**-H·PF_6 and **4·2**-H·PF_6 were exposed to an excess of acid, base, and water, in order to dissociate the V-shaped compounds from the dumbbell substrates.[11,13b] All resulting V·dumbbell mixtures were analysed by ^{1}H NMR spectroscopy from which the signals of the methylene protons adjacent to the dumbbell ammonium group (H_d, H_e, and H_d') as well as the aldehyde proton are compared (Fig. S4–S7†). The outcome for both the V·dumbbell complexes **4·1**-H·PF_6 and **4·2**-H·PF_6 after the same treatment, is somewhat similar (Table 5). After the addition of 10 equiv. of 3 M HCl to the V·dumbbell complex **4·1**-H·PF_6, the complex dissociates into its separate components **4** and **1**-H·PF_6 within 5 min, whereas the diimine **4** is only partially dissociated into the aldehyde and amine moieties (Fig. S4B†). Somewhat unexpectedly, the acid-promoted dissociation of the V·dumbbell complex **4·2**-H·PF_6 yields a fast exchange equilibrium mixture which contains both the averaged ^{1}H NMR signals between the V·dumbbell complex and the free dumbbell **1**-H·PF_6 (Fig. S6B†). The addition of base (Et_3N, 10 equiv.) to both V·dumbbell complexes after 5 min leads to subsequent deprotontation of the ammonium dumbbells, while **4** and the deprotonated dumbbells **1**/**2** become completely dissociated. Noticeably, diimine **4** is stable under such basic conditions (Fig. S5 and S7†). On the other hand, the mixture of the V·dumbbell complexes with a large excess of water (D_2O, 200 equiv.) requires almost an hour to reach equilibrium, whereas the complexes and the V-shaped compounds only undergo partial dissociation (Fig. S4C and S6C†).

Fluorescent properties of the anthracene-containing dumbbell compound **2**-H·PF_6 in the presence of acid, base, and water have been reported as a comparison in the present study.[11] Mixtures of the anthracene-containing V·dumbbell complex **4·2**-H·PF_6 treated separately with acid (3 M HCl, 10 equiv.), base (Et_3N, 10 equiv.) and water (200 equiv.), were analysed (Fig. 6, Table 5) by fluorescence spectroscopy with an excitation wavelength of 290 nm and a fixed dumbbell concentration at 0.02 mM. By monitoring the anthracene fluorescence intensity (λ_{max} = 418 nm) in the equilibrium mixture of the reactants and products, we can estimate the V·dumbbell complex concentration. The fluorescence spectrum of the V·dumbbell complex **4·2**-H·PF_6 treated with acid reveals (Fig. 6A) the characteristic anthracene emission of pure [**2**-H]$^+$. The fluorescence spectrum

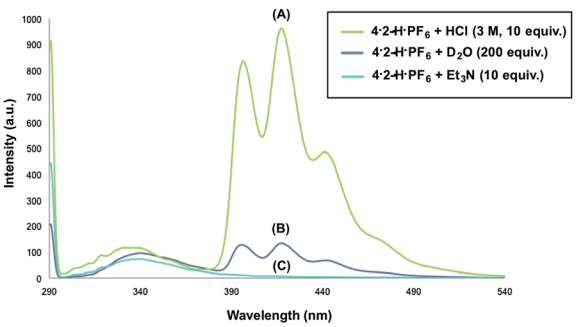

Fig. 6 Fluorescence emission spectra (excitation wavelength = 290 nm) of the V·dumbbell mixture **4·2**-H·PF_6 after addition of (A) acid, (B) water, and (C) base (fixed dumbbell concentration at 0.02 mM in 9 : 1 CH_2Cl_2–MeCN).

Table 5 The outcome of **4·1**-H·PF_6 (left) and **4·2**-H·PF_6 (right) and the V·dumbbell complexes (20 mM, CD_2Cl_2/CD_3CN 9 : 1) upon addition of excess of acid, base, and water, characterised by ^{1}H NMR spectroscopy. "1" represents the presence of the output substrate while "0" represents the absence of the output substrate

	Input				Input		
Output	Acid[a]	Base[b]	Water[c]	Output	Acid[a]	Base[b]	Water[c]
4·1-H·PF_6	0	0	1	**4·2**-H·PF_6	1	0	1
1-H·PF_6	1	1[d]	1	**2**-H·PF_6	1	1[d]	1
4	1	1	1	**4**	1	1	1
p-Isopropyl aniline	1	0	1	*p*-Isopropyl aniline	1	0	1
2,6-Diformyl pyridine	1	0	1	2,6-Diformyl pyridine	1	0	1
Fluorescence[e]	0	0	0	Fluorescence[e]	1	0	1

[a] HCl (3 M, 10 equiv.), NMR spectrum obtained after 5 min of acid addition, final conc. = 18.7 mM. [b] Et_3N (10 equiv.), NMR spectrum 5 min after base addition, final conc. = 19.5 mM. [c] D_2O (200 equiv.), NMR spectrum obtained after 1 h of water addition, final conc. = 18.6 mM. [d] In deprotonated form. [e] Fluorescence intensity > 50 a.u. with a λ_{max} of 418 nm.

of **4**·**2**-H·PF_6 treated with water demonstrates (Fig. 6B) the characteristic anthracene emission, yet with an intensity of 15%. Therefore, the dissociation of V·dumbbell complex **4**·**2**-H·PF_6 in the aqueous solution is incomplete. In contrast, the fluorescence spectra of **4**·**2**-H·PF_6, after treatment with base reveals (Fig. 6C) complete fluorescence quenching of the anthracene emission. This result reflects the fact that the covalently linked secondary amine of the deprotonated dumbbell **2** deactivates the lower-lying anthracene fluorescence.

As a result, the V·dumbbell complexes possess relative stabilities toward hydrolysis in the presence of a large excess of water. Generally, rapid and complete dissociation of the V·dumbbell complexes can be achieved on addition of acid (complex **4**·**2**-H·PF_6 requires large excess of acid) or base. The resulting substrates could be isolated by column chromatography. When a cationic polymer substrate is employed, eventually, the polymer substrate can be purified by a simple precipitation in a specific solvent system wherein the V-shaped molecular components are soluble.

3. Conclusions

A series of diimine V-shaped compounds **3–9** with different *para*-substituents (R = OMe, ^{i}Pr, Me, H, Cl, F, and CF_3) on the terminal aromatic rings have been prepared for complexation with two dumbbell substrates. Single crystals of the V-shaped compounds **3**, **5**, and **8**, as well as the dumbbell **2**-H·PF_6 have been obtained and subjected to X-ray structure determination. The self-assembly binding mode of the V·dumbbell complexes was evaluated by ^{1}H NMR spectroscopy. The binding constants and stoichiometries between the V-shaped compounds and the dumbbells were determined using the Method of Continuous Variations and the Rose-Drago Method based on ^{1}H NMR spectroscopic data. Within the series of V-shaped compounds, the binding strengths with both dumbbells weaken with the decreasing electron-donating ability of the R substituents. Moreover, the V-shaped compound **4** shows a stronger binding with the symmetrical dumbbell **1**-H·PF_6 than with the unsymmetrical anthracene-containing dumbbell **2**-H·PF_6. Fluorescence measurement of equimolar mixtures of **3–9** and the dumbbell **2**-H·PF_6 caused reduced anthracene emission by approximately 50%, showing that the complexes formed could not completely quench the anthracene fluorescence. Rapid (<5 min) and complete dissociation of the V-shaped compounds from the dumbbells could be realised by using an excess of acid or base, whereas only partial dissociation of the complexes was observed (<1 h) with a large excess of water. Further exploration of these complexes with fluorinated dumbbells[22] may give enhanced bindings. Such modifications may potentially lead to rapid and controlled functionalisation/disfunctionalisation of polyelectrolyte materials,[23] and their acting as a gate-switchable part at the surface of nanoparticles.[24]

4. Experimental section

General methods

1-H·PF_6, **2**-H·PF_6, **3**, **5**, and **6** are known compounds which were synthesised and characterised according to literature procedures.[11,13b,17] Compounds **4**, **7**, **8**, and **9** have not been reported in the literature before. All non-aqueous reactions were carried out under dry, high-purity N_2 with oven-dried (115 °C) glassware. Unless otherwise specified, all solvents and reagents were purchased commercially and used without further purification. Dichloromethane (CH_2Cl_2) was freshly distilled from CaH_2. Acetonitrile (MeCN) was pre-dried by stirring with CaH_2 for 24 h and distillation under N_2, and stored in the presence of molecular sieves (4 Å). Thin layer chromatography (TLC) was performed on silica gel 60 F_{254} (Merck). Melting points were measured on an Electrothermal 9100 digital melting point apparatus and are uncorrected. UV/visible absorption spectra were obtained using a Cary 5 G UV/visible/NIR spectrophotometer. Excitation and fluorescence spectra were recorded using a Hitachi F-4500 Fluorescence spectrophotometer. ^{1}H, ^{13}C, and ^{1}H NOESY NMR spectra for structural characterization were recorded on Bruker Avance 400 (^{1}H: 400 MHz; ^{13}C: 101 MHz) spectrometer at 296 K. NMR samples were dissolved in CD_2Cl_2 unless otherwise stated. Chemical shifts were reported as parts per million (ppm) on the δ scale and calibrated by using the solvent residual peak as internal standard. Coupling constants (J) are reported in Hertz. Electrospray ionization (ESI) mass spectra were obtained on a Thermo Finnigan MAT 95XL mass spectrometer using 1 : 1 CH_2Cl_2–MeOH as the mobile phase. The reported m/z values correspond to the most abundant monoisotopic masses. X-ray diffraction data of crystalline compounds were collected with a Bruker APEX II diffractometer or a Bruker ASX CCD X-ray system.

General procedure for synthesising diimine V-Shaped compounds

A solution of the *p*-substituted aniline (2.0 equiv.) and 2,6-diformylpyridine (1.0 equiv.) in anhydrous CH_2Cl_2 (1 mL $mmol^{-1}$) was stirred in the presence of molecular sieves (4 Å) for 4 h. The molecular sieves were filtered off and washed with CH_2Cl_2. The excess of solvent in the filtrate was removed under vacuum to yield the product.

3 (R = OMe)

Slow vapour diffusion of ^{t}BuOMe into a solution of **3** in $ClCH_2CH_2Cl$ yielded single crystals (colourless prisms, 0.40 × 0.30 × 0.20 mm) suitable for X-ray crystallography. Crystal data: $[C_{21}H_{19}N_3O_2]$, M = 345.39, orthorhombic, *Aba2*, a = 7.1660(6), b = 40.204(3), c = 6.3427(5) Å, $\alpha = \beta = \gamma = 90°$, V = 1827.4(3) Å^3, Z = 4, D_{calcd} = 1.255 mg m^{-3}, μ(Mo-K_α) = 0.083 mm^{-1}, $F(000)$ = 728, T = 296 K, 2019 independent measured reflections, full-matrix least-squares on F^2 refinement, R_1 = 0.0439, wR_2 = 0.0920, 1226, independent observed reflections, [$|F_o| > 4\sigma(|F_o|)$, $2\theta_{max} = 55.9°$], 119 parameters. CCDC code: 784762.

4 (R = ^{i}Pr)

Following the general procedure, a mixture of 4-isopropylaniline (0.49 g, 3.60 mmol) and 2,6-diformylpyridine (0.24 g, 1.80 mmol) was stirred in anhydrous CH_2Cl_2 (5 mL) with molecular sieves (4 Å) for 4 h. On filtration and removal of the solvent, the diimine **4** was obtained as a bright yellow solid

(0.55 g, 83%). R_f: 0.81 (hexane–EtOAc = 1 : 1). M.p. 126.8–127.2 °C. ^{1}H NMR (CD_2Cl_2): 1.28 (d, J = 6.9 Hz, 12H, $CH(CH_3)_2$), 2.96 (quin, J = 6.9 Hz, 2H, $CH(CH_3)_2$), 7.26–7.34 (m, 8H, Ar*H*), 7.94 (t, J = 7.8 Hz, 1H, Ar*H*), 8.27 (d, J = 7.8 Hz, 2H, Ar*H*), 8.68 (s, 2H, *H*C = N). ^{13}C NMR (CD_2Cl_2): 24.4, 34.3, 121.7, 123.2, 127.8, 137.8, 148.6, 149.1, 155.4, 159.9. HRMS (MALDI-TOF): $C_{32}H_{27}N_3$ $[M + Na]^+$: calcd 392.2097; found 392.2100.

5. (R = Me)

Slow vapour diffusion of MeCN into a solution of **5** in CH_2Cl_2 yielded single crystals (colourless prisms, 0.50 × 0.40 × 0.30 mm) suitable for X-ray crystallography. Crystal data: $[C_{21}H_{19}N_3]$, M = 313.39, monoclinic, $P2/c$, a = 4.7249(7), b = 6.2811(9), c = 28.965(4) Å, α = 90, β = 94.639(3), γ = 90, V = 856.8(2) Å^3, Z = 2, D_{calcd} = 1.215 mg m^{-3}, μ(Mo-K_α) = 0.073 mm^{-1}, $F(000)$ = 332, T = 296 K, 1566 independent measured reflections, full-matrix least-squares on F^2 refinement, R_1 = 0.1810, wR_2 = 0.6184, 1391, independent observed reflections, [$|F_o| > 4\sigma(|F_o|)$, $2\theta_{max}$ = 50.5°], 111 parameters. CCDC code: 784763.

7 (R = Cl)

Following the general procedure, a mixture of 4-chloroaniline (0.33 g, 2.60 mmol) and 2,6-diformylpyridine (0.18 g, 1.30 mmol) was stirred in anhydrous CH_2Cl_2 (4 mL) with molecular sieves (4 Å) for 4 h. On filtration and removal of the solvent, the diimine **7** was obtained as a yellow powder (0.66 g, quantitative). R_f: 0.59 (hexane–EtOAc = 1 : 1). M.p. > 198.4 °C (decomposed). ^{1}H NMR (CD_2Cl_2): 7.27 (d, J = 8.7 Hz, 4H, Ar*H*), 7.41 (d, J = 8.7 Hz, 4H, Ar*H*), 7.97 (t, J = 7.8 Hz, 1H, Ar*H*), 8.29 (d, J = 7.8 Hz, 2H, Ar*H*), 8.63 (s, 2H, *H*C = N). ^{13}C NMR (CD_2Cl_2): 123.1, 123.7, 129.9, 132.8, 138.0, 150.0, 155.1, 161.2. HRMS (MALDI-TOF): $C_{19}H_{13}Cl_2N_3$ $[M + Na]^+$: calcd 376.0376; found 376.0378.

8 (R = F)

Following the general procedure, a mixture of 4-fluoroaniline (0.30 g, 2.72 mmol) and 2,6-diformylpyridine (0.18 g, 1.36 mmol) was stirred in anhydrous CH_2Cl_2 (4 mL) with molecular sieves (4 Å) for 4 h. On filtration and removal of the solvent, the diimine **8** was obtained as a light yellow powder (0.27 g, 62%). R_f: 0.72 (hexane–EtOAc = 1 : 1). M.p. 172.3–173.0 °C. ^{1}H NMR (CD_2Cl_2): 7.10–7.18 (m, 4H, Ar*H*), 7.29–7.37 (m, 4H, Ar*H*), 7.95 (t, J = 7.8 Hz, 1H, Ar*H*), 8.27 (d, J = 7.8 Hz, 2H, Ar*H*), 8.64 (s, 2H, *H*C = N). ^{13}C NMR (CD_2Cl_2): 116.4, 116.6, 123.3, 123.4, 123.4, 137.9, 147.46, 147.49, 155.2, 160.52, 160.53, 161.1, 163.6. HRMS (MALDI-TOF): $C_{19}H_{13}F_2N_3$ $[M + Na]^+$: calcd 344.0970; found 344.0965. Slow vapour diffusion of ^{t}BuOMe into a solution of **8** in $ClCH_2CH_2Cl$ yielded single crystals (yellow prisms, 0.50 × 0.40 × 0.30 mm) suitable for X-ray crystallography. Crystal data: $[C_{19}H_{13}N_3F_2]$, M = 321.32, monoclinic, $C2/c$, a = 35.041(6), b = 6.2652(11), c = 7.1363(12) Å, α = 90, β = 92.850(3), γ = 90, V = 1564.7(5) Å^3, Z = 4, D_{calcd} = 1.364 Mg m^{-3}, μ(Mo-K_α) = 0.099 mm^{-1}, $F(000)$ = 664, T = 296 K, 5197 independent measured reflections, full-matrix least-squares on F^2 refinement, R_1 = 0.0607, wR_2 = 0.1442, 1407, independent observed reflections, [$|F_o| > 4\sigma(|F_o|)$, $2\theta_{max}$ = 50.5°], 110 parameters. CCDC code: 798464.

9 (R = CF$_3$)

Following the general procedure, a mixture of 4-trifluoromethyl aniline (0.37 g, 2.28 mmol) and 2,6-diformylpyridine (0.15 g, 1.14 mmol) was stirred in anhydrous CH_2Cl_2 (3 mL) with molecular sieves (4 Å) for 4 h. On filtration and removal of the solvent, the diimine **9** was obtained as an off-white powder (0.54 g, quantitative). R_f: 0.68 (hexane–EtOAc = 1 : 1). M.p. 149.1–149.7 °C. ^{1}H NMR (CD_2Cl_2): 7.37 (d, J = 8.3 Hz, 4H, Ar*H*), 7.70 (d, J = 8.3 Hz, 4H, Ar*H*), 8.02 (t, J = 7.8 Hz, 1H, Ar*H*), 8.33 (d, J = 7.8 Hz, 2H, Ar*H*), 8.64 (s, 2H, *H*C = N). ^{13}C NMR (CD_2Cl_2): 121.8, 124.2, 125.2 (q, J = 215.5 Hz), 127.0 (m), 128.8 (q, J = 32.7 Hz), 138.1, 154.7, 154.9, 162.7. HRMS (MALDI-TOF): $C_{21}H_{13}F_6N_3$ $[M + H]^+$: calcd 422.1086; found 422.1095.

Dumbbell 2-H·PF$_6$

Slow vapour diffusion of ^{t}BuOMe into a solution of **2**-H·PF$_6$ in CH_2Cl_2 yielded single crystals (yellow prisms, 0.50 × 0.40 × 0.30 mm) of the dumbbell suitable for X-ray crystallography. Crystal data: $[C_{48}H_{48}N_2O_4]Cl(PF_6)$, M = 897.30, triclinic, $P\bar{1}$, a = 12.0530(4), b = 12.8073(4), c = 16.0081(9) Å, α = 95.8310(10), β = 99.9830(10), γ = 114.1490(10), V = 2179.41(16) Å^3, Z = 2, D_{calcd} = 1.367 Mg m^{-3}, μ(Mo-K_α) = 0.197 mm^{-1}, $F(000)$ = 936, T = 296 K, 7855 independent measured reflections, full-matrix least-squares on F^2 refinement, R_1 = 0.0420, wR_2 = 0.1117, 6456, independent observed reflections, [$|F_o| > 4\sigma(|F_o|)$, $2\theta_{max}$ = 50.5°], 562 parameters. CCDC code: 784761.

Acknowledgements

This research was supported by a General Research Fund (201412) awarded by the Hong Kong Research Grants Council, and a grant from the University Grants Committee of Hong Kong SAR (AoE/P-03/08).

References

1 C.-W. Chen and H. W. Whitlock, *J. Am. Chem. Soc.*, 1978, **100**, 4921–4922.
2 M. Hardouin-Lerouge, P. Hudhomme and M. Sallé, *Chem. Soc. Rev.*, 2011, **40**, 30–43 and references therein.
3 (*a*) X.-X. Peng, H.-Y. Lu, T. Han and C.-F. Chen, *Org. Lett.*, 2007, **9**, 895–898; (*b*) J. Cao, X.-Z. Zhu and C.-F. Chen, *J. Org. Chem.*, 2010, **75**, 7420–7423.
4 (*a*) S. C. Zimmerman and C. M. VanZyl, *J. Am. Chem. Soc.*, 1987, **109**, 7894–7896; (*b*) F.-G. Klärner and B. Kahlert, *Acc. Chem. Res.*, 2003, **36**, 919–932; (*c*) F. Marchioni, A. Juris, M. Lobert, U. P. Seelbach, B. Kahlert and F.-G. Klärner, *New J. Chem.*, 2005, **29**, 780–784.
5 Y. Kim and M. Park, *Synth. Met.*, 2001, **117**, 297–299.
6 J. Leblond, H. Gao, A. Petitjean and J.-C. Leroux, *J. Am. Chem. Soc.*, 2010, **132**, 8544–8545.
7 J. Cao, H.-Y. Lu, X.-J. You, Q.-Y. Zheng and C.-F. Chen, *Org. Lett.*, 2009, **11**, 4446–4449.
8 H. M. Colquhoun, Z. X. Zhu, C. J. Cardin, Y. Gan and M. G. B. Drew, *J. Am. Chem. Soc.*, 2007, **129**, 16163–16174.

9 (*a*) V. K. Potluri and U. Maitra, *J. Org. Chem.*, 2000, **65**, 7764–7769; (*b*) S. T. Weiss, N. R. Mclntyre, M. L. McLaughlin and D. J. Merkler, *Drug Discovery Today*, 2006, **11**, 819–824.

10 E. V. Tulyakova, G. Vermeersch, E. N. Gulakova, O. A. Fedorova, Y. V. Fedorov, J. C. Micheau and S. Delbaere, *Chem.–Eur. J.*, 2010, **16**, 5661–5671.

11 W.-Y. Wong, K. C.-F. Leung and J. F. Stoddart, *Org. Biomol. Chem.*, 2010, **8**, 2332–2343.

12 K. C.-F. Leung, C.-P. Chak, C.-M. Lo, W.-Y. Wong, S. H. Xuan and C. H. K. Cheng, *Chem.–Asian J.*, 2009, **4**, 364–381.

13 (*a*) K. C.-F. Leung, S. H. Xuan and C.-M. Lo, *ACS Appl. Mater. Interfaces*, 2009, **1**, 2005–2012; (*b*) K. C.-F. Leung, W.-Y. Wong, F. Aricó, P. C. Haussmann and J. F. Stoddart, *Org. Biomol. Chem.*, 2010, **8**, 83–89; (*c*) K. C.-F. Leung and K.-N. Lau, *Polym. Chem.*, 2010, **1**, 988–1000.

14 G. J. P. Britovsek, M. Bruce, V. C. Gibson, B. S. Kimberley, P. J. Maddox, S. Mastroianni, S. J. McTavish, C. Redshaw, G. A. Solan, S. Strömberg, A. J. P. White and D. J. Williams, *J. Am. Chem. Soc.*, 1999, **121**, 8728–8740.

15 K. S. Chichak, S. J. Cantrill, A. R. Pease, S.-H. Chiu, G. W. V. Cave, J. L. Atwood and J. F. Stoddart, *Science*, 2004, **304**, 1308–1312.

16 (*a*) A. Goswami, S. Sengupta and R. Mondal, *CrystEngComm*, 2012, **14**, 561–572; (*b*) M. A. Ramirez, A. M. Cuadro, J. Alvarez-Builla, O. Castano, J. L. Andres, F. Mendicuti, K. Clays, I. Asselberghs and J. J. Vaquero, *Org. Biomol. Chem.*, 2012, **10**, 1659–1669; (*c*) P.-C. Cheng, F.-S. Tseng, C.-T. Yeh, T.-G. Chang, C.-C. Kao, C.-H. Lin, W.-R. Liu, J.-S. Chen and V. Zima, *CrystEngComm*, 2012, **14**, 6812–6822; (*d*) S.-Q. Zhang, F.-L. Jiang, M.-Y. Wu, J. Ma, Y. Bu and M.-C. Hong, *Cryst. Growth Des.*, 2012, **12**, 1452–1463; (*e*) H. Zhou, G.-X. Liu, X.-F. Wang and Y. Wang, *CrystEngComm*, 2013, **15**, 1377–1388; (*f*) X.-G. Guo, W.-B. Yang, X.-Y. Wu, K. Zhang, L. Lin, R.-M. Yu and C.-Z. Lu, *CrystEngComm*, 2013, **15**, 3654–3663; (*g*) Q.-X. Yang, L.-F. Huang, M.-D. Zhang, Y.-Z. Li, H.-G. Zheng and Q.-Y. Lu, *Cryst. Growth Des.*, 2013, **13**, 440–445.

17 (*a*) P. T. Glink, A. I. Oliva, J. F. Stoddart, A. J. P. White and D. J. Williams, *Angew. Chem., Int. Ed.*, 2001, **40**, 1870–1875; (*b*) M. Horn, J. Ihringer, P. T. Glink and J. F. Stoddart, *Chem.–Eur. J.*, 2003, **9**, 4046–4054; (*c*) F. Aricó, T. Chang, S. J. Cantrill, S. I. Khan and J. F. Stoddart, *Chem.–Eur. J.*, 2005, **11**, 4655–4666.

18 G. A. Jeffrey, *An Introduction to Hydrogen Bonding*, Oxford University Press, Oxford, U. K., 1997, ch. 4.

19 (*a*) K. C.-F. Leung, F. Aricó, S. J. Cantrill and J. F. Stoddart, *J. Am. Chem. Soc.*, 2005, **127**, 5808–5810; (*b*) K. C.-F. Leung, F. Aricó, S. J. Cantrill and J. F. Stoddart, *Macromolecules*, 2007, **40**, 3951–3959.

20 V. M. S. Gil and N. C. Oliveira, *J. Chem. Educ.*, 1990, **67**, 473–478.

21 *Analytical Methods in Supramolecular Chemistry*, ed. C. A. Schalley, Wiley-VCH, Weinheim, Germany, 2007, pp. 17–54.

22 (*a*) T. D. Nguyen, K. C.-F. Leung, M. Liong, C. D. Pentecost, J. F. Stoddart and J. I. Zink, *Org. Lett.*, 2006, **8**, 3363–3366; (*b*) K. C.-F. Leung, T. D. Nguyen, J. F. Stoddart and J. I. Zink, *Chem. Mater.*, 2006, **18**, 5919–5928.

23 C. R. South, K. C.-F. Leung, D. Lanari, J. F. Stoddart and M. Weck, *Macromolecules*, 2006, **39**, 3738–3744.

24 (*a*) R. Casasús, E. Climent, M. D. Marcos, R. Martínez-Máñez, F. Sancenón, J. Soto, P. Amorós, J. Cano and E. Ruiz, *J. Am. Chem. Soc.*, 2008, **130**, 1903–1917; (*b*) J. F. Stoddart, *Angew. Chem., Int. Ed.*, 2012, **51**, 12902–12903; (*c*) P. R. McGonigal and J. F. Stoddart, *Nat. Chem.*, 2013, **5**, 260–262.

